This article has been published in Nanotechnology. The final publication is available on IOP Science doi: 10.1088/1361-6528/ab0444

Fabrication of polycaprolactone electrospun nanofibers doped with silver nanoparticles formed by air plasma treatment

Dakota M. Binkley[1], Bryan E.J. Lee[2], Sokunthearath Saem[3], Jose Moran-Mirabal[2,3], and Kathryn Grandfield [1,2]

1. Department of Materials Science and Engineering, McMaster University, Hamilton, ON, Canada, L8S 4K1

2. School of Biomedical Engineering, McMaster University, Hamilton, ON, Canada, L8S 4K1

3. Department of Chemistry and Chemical Biology, McMaster University, Hamilton, ON, Canada, L8S 4K1

Abstract

Implanted devices are prone to bacterial infections, which can result in implant loosening and device failure. Mitigating these infections is important to both implant stability and patient health. The development of antibacterial implant coatings can decrease the presence of bacterial colonies, reducing the risk for bacterial-dependent implant failure. Here, we show that electrospun polycaprolactone (PCL) fibers doped with silver nanoparticles (NPs) from a silver nitrate precursor have the potential to decrease the prevalence of *Streptococcus pneumoniae* (*S. pneumoniae*) while supporting osteoblast attachment and proliferation. An air plasma reduction method of PCL electrospun fibers was used to prepare fibers doped with silver NPs. Fibers were characterized using scanning electron microscopy (SEM) and transmission electron microscopy (TEM) for qualitative evaluation of NP distribution and quantitative analysis of fiber diameters. Antibacterial testing against *S. pneumonia* was performed with successful inhibition observed after 24 hours of exposure. *In vitro* testing was completed using Saos-2 cells and suggests that the negative surface charge has the potential to increase mammalian cell viability even in the presence of fibers containing NPs. In conclusion, this study describes a novel method to produce a bioresorbable implant coating with the ability to reduce bacterial infections surrounding the implant surface while remaining biocompatible to the host.

Keywords: polycaprolactone, silver nanoparticles, antimicrobial, dental implant, osseointegration, air plasma treatment, electrospinning

Introduction

Over 4.4 million Americans have at least one internal fixation device (i.e. dental or orthopedic implant)[1]. The short-term success of these implants relies on bone-implant osseointegration: the structural and functional connection of bone to the implant surface[2].

However, long-term implant success also relies on the host's immune system – if a patient develops a bacterial infection surrounding the implant site, they can face hospitalization, or implant loosening [1]. Colonization of *Staphylococci* and other bacteria can result in both a harmful infection and a decrease in implant longevity[3]. Traditional techniques used to combat post-operational infections at implant surfaces, such as antibiotic prophylaxis have demonstrated limited success[1]. The notion of eliminating bacterial infections at the source, using nanotechnology instead of large doses of antibiotics could be more beneficial to both the patient's health and implant longevity [1,4].

Silver nanoparticles (NPs) are well characterized antimicrobial agents, which have been shown to successfully inhibit gram-positive and gram-negative bacterial colonies[5]. The complete mechanism for silver NP antimicrobial activity is still debated; however, it is understood that the small particles can penetrate the bacterial membrane[6,7]. Once silver NPs have entered the cell, they can interact with various organelles and intracellular fluid can leak from the holes created by the NPs in the cell membrane. Additionally, the silver oxidizes upon entry to Ag^{+} ions that can to bind to bacterial DNA. The resulting conformational changes lead to the corruption of protein structure and ultimately cell death[7,8]. The success of silver NPs as antimicrobial agents has the potential to decrease the rate of bacterial infection at the bone-implant interface.

A commonly proposed method to deliver silver NPs to an individual is to utilize an antimicrobial scaffold [9–14]. Polycaprolactone (PCL) has been demonstrated to be both biologically compatible and acceptable for human implantation which gives it numerous potential biomedical applications [15–17]. Electrospinning is a popular method used to create three-dimensional porous scaffolds that can mimic extracellular matrices (ECMs) due to their similar topology and morphology [18]. In addition, electrospun nanofibers can be functionalized such that they can deliver site-specific drugs, or biocompatible agents [19]. For instance, hydroxyapatite has been electrospun with biocompatible polymers such as PCL and polyvinyl alcohol to improve osteoblast cell adhesion [20]. Drugs, including coagulants can also be electrospun with polymers such that site specific delivery can occur [21]. Electrospinning of PCL has become a popular method to create scaffolds that can assist in tissue regeneration, wound healing, and drug delivery [17]. This method has also been seamlessly adapted for the coating of titanium implants, with different alloyed

compositions, to improve osseointegration [22–24].Cellular recognition and viability on titanium implant surfaces has increased with PCL coatings [22–24]. Meanwhile, blended PCL coatings have also demonstrated an increase of bioactive properties of titanium implants through cell viability assays [20].

Silver NPs have been successfully incorporated onto PCL nanofibers either by surface functionalization or pre-loading (the addition of silver NPs prior to electrospinning) and have demonstrated antimicrobial success [10,11]. However, these methods require an additional step to produce silver NPs for incorporation or attachment. Direct incorporation of a silver nitrate solution during electrospinning, and one-step conversion to silver NPs is a simpler approach that could be achieved using plasma treatment of as-spun fibers. Argon plasma treatment has demonstrated NP formation on chitosan fibers [25], yet simpler air plasma treatment has yet to be utilized to form silver NPs on PCL fibers. An advantage to this method of NP formation is the decrease in fiber diameter observed, allowing production of fibers that more closely mimic the native ECM while displaying antibacterial properties. This study discusses the fabrication and characterization of PCL electrospun nanofibers with air plasma treated silver NPs. The fiber fabrication method has been optimized by varying the quantity of the NP precursor ($AgNO_3$) and varying plasma treatment times. The morphology, antimicrobial activity, and cytocompatibility of these fibers were subsequently evaluated.

Materials and Methods

PCL Solution Preparation

8 wt%, 9 wt%, and 12 wt% PCL (MW 80 000, Sigma Aldrich, St. Louis, MO) solutions were prepared using acetone (Sigma Aldrich, HPLC 99.9%, St. Louis, MO) as the solvent. The solutions were heated to 40°C and mixed until fully dissolved.

Electrospinning Optimization

A syringe pump (Harvard Apparatus, QC, Canada), voltage supply (Spellman, Valhalla, NY), and collector were used to create a closed grounded circuit. The PCL solution was ejected from a 1 mL plastic syringe (BD Syringes, USA) equipped with a 22G needle tip at various flow rates, tip to collector distances (TCDs), voltages, and solution concentrations until conditions were optimized (Figure S1). The tested conditions included TCDs that from 7 to 17.5 cm, voltages from 10 to 20 kV, and solution concentrations from 8 to 12 wt% PCL. The optimized conditions were flow rate of 0.1 mL/min at a TDC of 9
cm, a voltage of 19 kV, and a solution concentration of 12 wt% PCL. These conditions were used in all reported experiments.

Fabrication of PCL/Silver NP Scaffolds

PCL was dissolved in acetone at 12 wt%, as described above, and silver nitrate (Sigma

Aldrich, St. Louis, MO) was added in varying amounts (1, 2.5, 5, and 10 wt% relative to PCL mass) to the solutions. Scaffolds were electrospun using the optimized conditions onto the appropriate material for subsequent testing described below. The scaffolds were air plasma treated using a PDC001 Expanded Plasma Cleaner (Harrick Plasma, Ithaca, NY) at an air flow rate of 600 sccm for 1, 5, 10, and 30 minutes to reduce the $AgNO_3$ and create surface immobilized silver NPs [25]. Fibers were then rinsed with water for 15 minutes and air-dried. Plasma treatment times of 1 to 30 min are abbreviated in the text as PT 1, PT 5, PT 10, PT 30.

Fiber Surface Treatment

Prior to antimicrobial and *in vitro* testing, fibers were immersed with 0.1 M NaOH solution for 24 hours to increase the surface wettability and induce a negative surface charge[26]to enhance cell growth. After NaOH submersion, fibers were rinsed with Milli-Q water twice.

Characterization

Fibers were imaged using scanning electron microscopy (SEM) on a JEOL 7000F (JEOL Canada, Ltd., Montreal, QC) with an acceleration voltage of 2.5 kV. Prior to imaging, samples were sputter coated with carbon for 30 seconds to improve conductivity. A 12 wt% PCL solution containing 2.5wt% $AgNO_3$ was electrospun directly onto 500 mesh spacing uncoated TEM grids for five seconds. Fibers were subsequently air plasma treated for 10 minutes. Fibers were imaged using the JEOL 1200 TEMSCAN (JEOL Canada, Ltd., Montreal, QC) with an acceleration voltage of 80kV. Energy dispersive X-ray spectroscopy (EDS) was completed in the TEM to further confirm the presence of Ag.

Fiber Analysis

SEM images were analyzed using ImageJ software (National Institutes of Health)[27] to calculate average fiber diameter. All statistical analysis was performed using R (R Core Team, New Zealand). Statistical analysis was performed using a two-way ANOVA at a significance of $\alpha = 0.05$ which was followed by a Tukey's honestly significant difference (HSD) test. SEM images of approximately 100 μm^2 area of the 5 wt% $AgNO_3$ fiber using ImageJ software (National Institutes of Health) [27] to determine the percent surface area coverage of Ag and PCL, to provide an estimate of electrospun fiber composition, as this fiber composition is used for biocompatibility testing.

Antimicrobial Testing

12 wt% PCL solutions containing 5wt% silver nitrate were electrospun directly onto the collector plate. The fibrous meshes were removed, and samples were air plasma treated for 0 or 5 minutes. A subset of the fibers were also rinsed with NaOH for 24 hours and subsequently rinsed twice with water. A control PCL solution was electrospun directly onto the collector plate and not air plasma treated. The meshes were imaged in cross-section in the SEM and the thickness was determined to be 660± 30.0 μm (images not shown). The meshes were cut into 1 x 2 cm rectangles and subsequently UV

sterilized (wavelength 254 nm) for 15 minutes on each side as previously described[28].The area of inhibition was measured using ImageJ software (National Institutes of Health) [27].All statistical analysis was performed using R (R Core Team, New Zealand). Statistical analysis was performed using a one-way ANOVA at a significance of $\alpha = 0.05$ which was followed by a Tukey's HSD test. An *in vitro* antimicrobial activity analysis was completed on the scaffolds using wild type *Streptococcus pneumoniae* (*S. pneumoniae*) (ATCC®, USA). The bacteria were cultured in LB broth that was prepared by mixing 25 g of LB powder (EMD Millipore, USA) and purified water to a final volume of 1L. This solution was subsequently autoclaved on a liquid cycle at 121°C. To culture the *S. pneumoniae*, a 1 mL cryovial of bacteria was thawed at room temperature and added to 4 mL of LB broth. The 5 mL bacterial suspension was then incubated at 37°C until the *S. pneumoniae* reached an optical density (OD_{600}) of 0.5 as measured at a wavelength of 600 nm. Bacterial stock and a 4-fold dilution solution were plated and fibrous meshes were placed on top and incubated at 37°C for 24 hours. Bacterial plates were imaged using a Nikon camera and radiuses of inhibition were assessed.

Live/Dead Staining

Saos-2, osteosarcoma, cells (ATCC®, USA) were grown as described in previous work [29]. Cells were seeded at 10,000 cells/cm^2 and grown for 24hrs on the following coatings on 15 mm diameter Ti disks: PCL only, 5 wt% $AgNO_3$ PT 5, and 5 wt% $AgNO_3$ PT 5 plus 1 day NaOH rinse. Prior to cell testing, the exposed fibers were UV sterilized (wavelength 254 nm) for 20 minutes. The cell viability of Saos-2 cells on the samples was assessed after 24 hours of growth using a Live/Dead kit (Molecular Probes, Oregon, USA), where the final concentration of the live and dead dye solution was, 2 µM calcein and 4 µM ethidium homodimer-1, respectively. The cell media was removed from the wells and 250 µL dye solution was added and incubated for 30 minutes. Samples were imaged using a fluorescence microscope (Nikon-Eclipse LV100N POL, equipped with a 10· objective and a Retiga 2000R CCD monochromatic camera (QImaging, Surrey, BC, Canada), and NIS Elements software (Nikon, Ottawa, Canada).

Fluorescence live/dead images were overlaid after the imaging process. The percent of live versus dead cells over approximately 0.4 cm^2 area was completed using the particle analyzer after applying a colour threshold in ImageJ software (National Institutes of Health)[27].All statistical analysis was performed using R (R Core Team, New Zealand). Statistical analysis was performed using a two-way ANOVA at a significance of $\alpha = 0.05$ which was followed by a Tukey's HSD test.

Results

Fiber Fabrication and Characterization

In order to create a functional implant coating, the fabrication process was optimized to generate continuous PCL fibers. Continuous fibers were not observed with 8 – 10 wt%

PCL solutions, as significant spraying was visible (Figure S1). PCL solutions of 12 wt% had a visible Taylor cone and were further optimized. Optimal electrospinning conditions were determined to be a 12 wt% PCL solution in acetone, electrospun at 19 kV, at a TCD of 9 cm and a flow rate of 0.1 mL/min.

To successfully incorporate silver NPs into the scaffolds a NP precursor, silver nitrate, was added to the PCL/acetone solution prior to electrospinning. The addition of the precursor at various wt% compositions changed the properties of the PCL/acetone solution prior to electrospinning; however, no differences in fiber morphology were observed. To reduce the NP precursor to elemental silver, fibers were subjected to air plasma treatment for 1, 5, 10, or 30 minutes. SEM images confirm that continuous fibers were observed with air plasma treatment times of 1, 5 and 10 minutes (Figure 1). Images show that the fibers maintained structural integrity during the air plasma treatment at short time periods. However, after 30 minutes of treatment fibers were completely etched.

Fiber diameters were measured to determine if both precursor addition and subsequent air plasma treatment caused changes in the diameter (Figure 1E). As expected, there was a statistically significant reduction in fiber diameter with all increasing air plasma treatment times against the control PCL 0 wt% $AgNO_3$ fibers ($p < 0.05$). Interestingly, for the 1 wt%, 2.5 wt% and 5 wt% fibers, there was a significant reduction of fiber diameter when comparing those air plasma treated for 1 minute compared to both 5 and 10 minutes ($p < 0.05$). There was no significant difference found between the 5 and 10 minute air plasma treatment of these groups ($p < 0.05$). No significant reduction in fiber diameter was observed with increasing air plasma treatment of the 10 wt% preloaded group, indicating that increasing the amount of $AgNO_3$ added to the solution limits the diameter reduction. Moreover, the diameter reduction of the 0 wt % and 1 wt% groups appear to decrease in diameter linearly. In the other groups, this trend is not observed, further suggesting a reinforcement effect from the preloaded $AgNO_3$ and subsequent AgNPs.

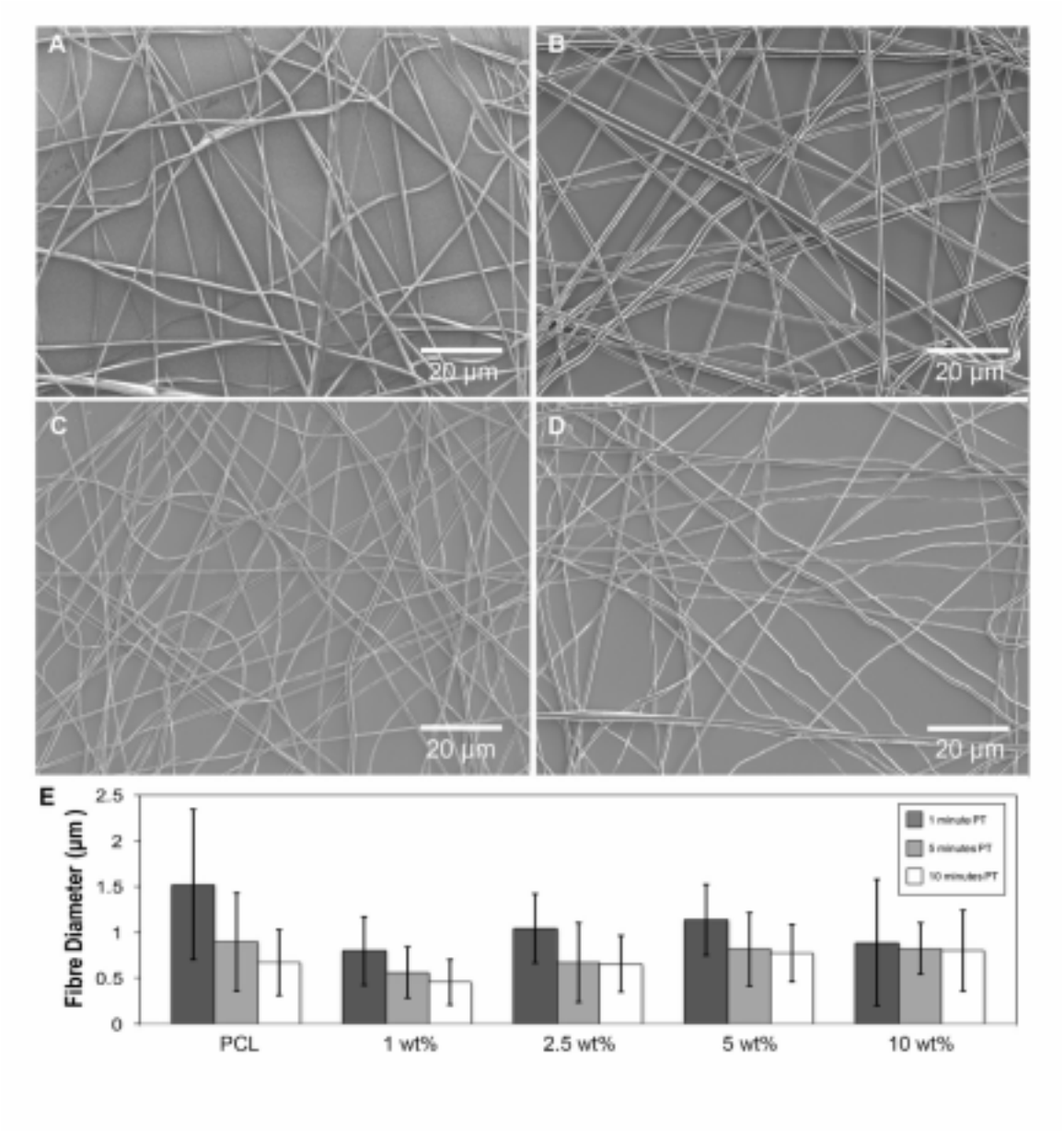

Figure 1.SEM images of continuous PCL fibers with various plasma treatment times. (A) PCL only control with no $AgNO_3$or plasma treatment. PCL nanofibers loaded with 5wt% $AgNO_3$ and plasma treatments of (B) 1, (C) 5 and (D) 10 minutes. Fibers were electrospun in a thin layer for more accurate diameter measurements. Thicker mats were obtained with longer electrospinning times. All images were taken at the same magnification. (E) Measured fiber diameters for scaffolds composed of PCL fibers loaded with various amounts of silver nitrate (0, 1, 2.5, 5, and 10 wt% $AgNO_3$) and with different plasma treatment times (1, 5, and 10 minutes). A clear trend of decreasing fiber diameter with increasing plasma treatment time is present in all but the 10 wt% $AgNO_3$ fibers. PT = plasma treatment time, error bars represent standard deviations, n = 50.

The addition of the silver nanoparticle precursor and subsequent air plasma treatment produced nanoparticles visible on the surface of the scaffolds (Figure 2). A high and

uniform density of Ag NP aggregates were observed along the fiber surfaces. EDS spectra confirmed the presence of Ag in the sample (Figure S2). TEM images suggest that the nucleated NPs are on average 7 ± 4 nm in diameter after 10 minutes of air plasma treatment. Fiber edges appear to be damaged at higher magnification; however, it is unclear if this is a result of air plasma treatment or TEM beam damage. Surface analysis of the 5 wt% $AgNO_3$ fibers demonstrated that the final electrospun fiber is comprised of approximately 7.7 ± 0.06 % Ag. Quantification of the composition was completed using SEM images, and therefore the NPs revealed in the TEM images were not accounted for. Therefore, the estimate of the final fiber composition is slightly lower than the actual composition.

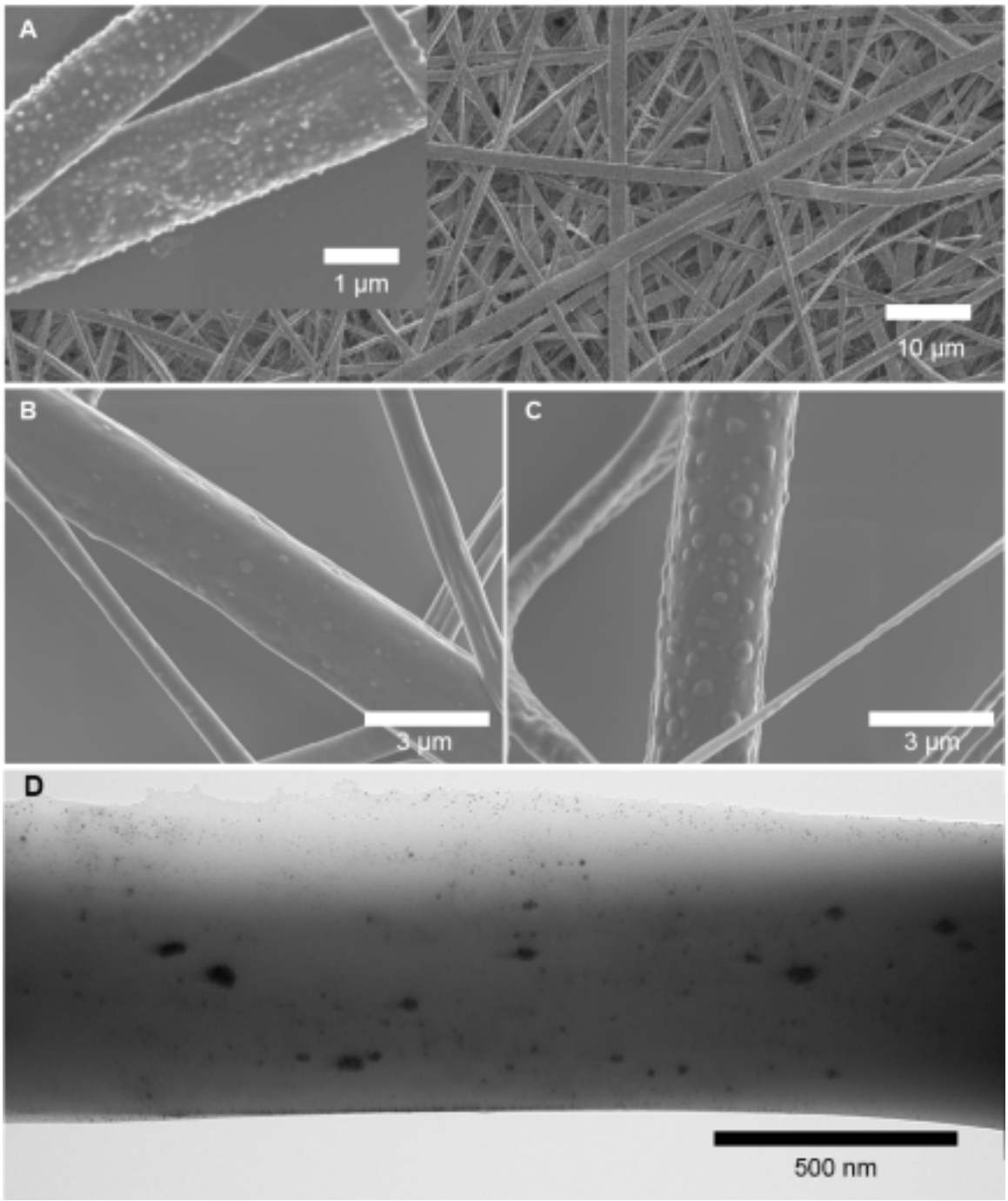

Figure 2. Silver nanoparticle characterization. SEM images of PCL fibers containing 5wt% $AgNO_3$and air plasma treated for (A) 5 minutes, where in lower magnifications Ag aggregates are not visible, but the higher magnification inset shows uniform Ag aggregates distributed across the isolated fibers, representative of most fibers. Higher magnification images of PCL fibers containing 5wt% $AgNO_3$and air plasma treated for(B) 1 and (C) 5 mins show silver NP aggregates on the fiber surfaces. Aggregates and smaller NPs are present on the fiber surface when observed by (C) TEM of PCL fibers containing 2.5 wt% $AgNO_3$and air plasma treated for 10 mins.

Fibers rinsed with 0.1 M NaOH for 24 hours exhibited randomly distributed, irregular

features across the surface which were identified using SEM (Figure 3). Fibers seem to merge together, making the surface appear to be rougher in some areas, which can be attributed to alkaline degradation of PCL [30,31]. This change in morphology appears to make the fibers inhomogeneous overall, which can also increase cellular attachment to the scaffold surface.

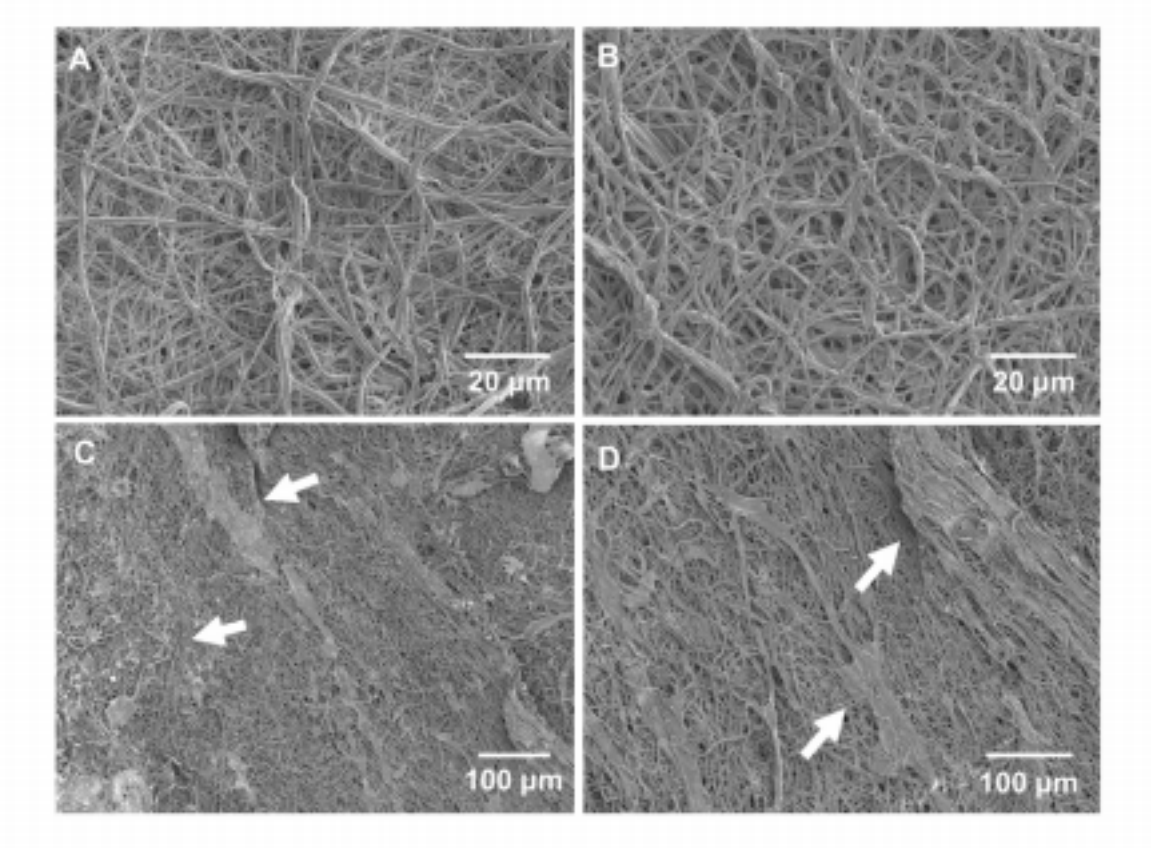

Figure 3. Impact of NaOH wash on fiber morphology. SEM images of mats of thick PCL (A) control fibers and (B) 5 wt% $AgNO_3$ PT 5 treated with 0.1 M NaOH for 1 day to (C, D) 5 wt% $AgNO_3$ PT 5 fibers treated for 1 day with 0.1 M NaOH at a lower magnification to demonstrate the many areas with changes in morphology, with evident features denoted by the white arrow.

Antibacterial Testing

The fibers were further investigated for their antimicrobial properties against *S. pneumoniae*. Fiber mats were placed directly onto *S. pneumoniae* colonies and incubated for 24 hours to determine if colonies could establish while in contact with the fibers (Figure 4). The area of inhibition was calculated to determine the antimicrobial capacity of the

fibers. S. pneumoniae grew effectively while in contact with the control PCL fibers as no inhibition was observed. However, S. pneumoniae growth was inhibited upon contact with the 5wt% AgNO3 PT 5 fibers, suggesting the nucleated NPs within the electrospun mats inhibited the S. pneumoniae, confirming the antimicrobial properties of the meshes (average effective area 2.1 ± 0.2 cm^2). To determine if the NaOH rinse decreased the efficacy of the antibacterial coating, 5 wt% $AgNO_3$ PT 5 fibers immersed in NaOH for 24 hours were also tested. These fibers had an average effective inhibition area of 1.8 ± 0.1cm^2, which is comparable to the areas of inhibition for the 5wt% $AgNO_3$ PT 5 fibers ($p < 0.05$) without NaOH wash This shows that degradation of the PCL surface induced by the NaOH immersion did not increase the likelihood of bacterial colony formation or attachment. Therefore, the fibers are effective at inhibiting the growth of *S. pneumoniae* on contact irrespective of NaOH wash.

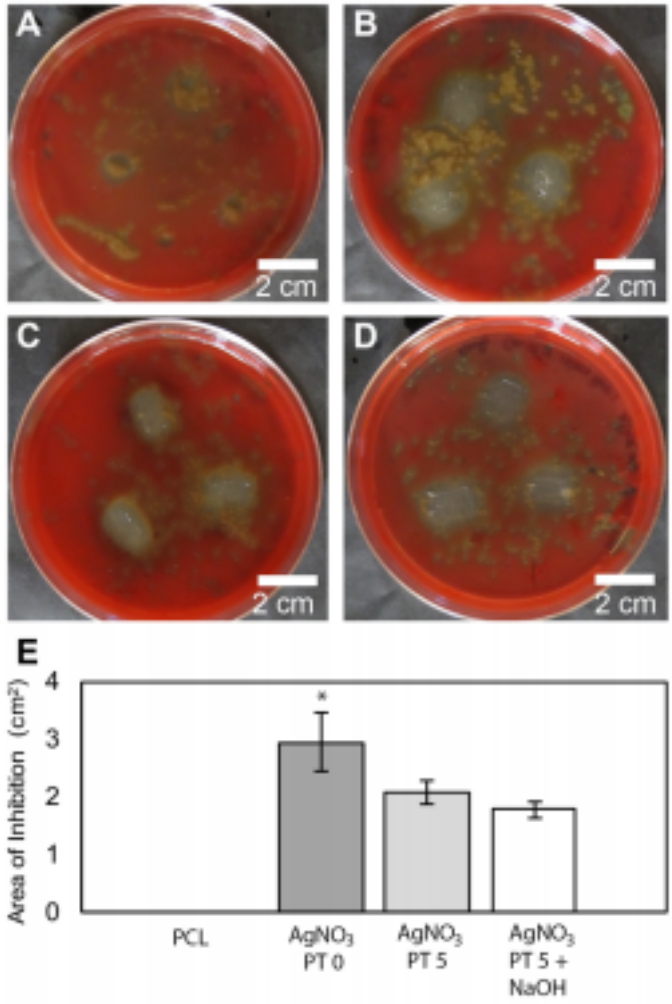

Figure 4. Culture plates showing the growth and inhibition of *S. pneumoniae* after 24 hours of interaction with the various fibers. (A) Control PCL fibers showed no inhibition; (B) 5 wt% $AgNO_3$ fibers with no PT (C) 5 wt% $AgNO_3$ PT 5 fibers and (D) 5 wt% $AgNO_3$ PT 5 fibers rinsed with NaOH for 24 hours. (E) Average areas of inhibition, error bars represent one standard deviation. 5 wt% $AgNO_3$ fibers with no PT had a significantly larger area of inhibition than all other tested fibers ($p < 0.05$). The 5 wt%

$AgNO_3$ PT 5 fibers and 5 wt% $AgNO_3$ PT 5 fibers rinsed with NaOH fibers had similar areas of inhibition ($p < 0.05$).

Live/Dead Staining

The Saos-2 cells were characterized using a Live/Dead stain and fluorescence microscopy, where live and dead cells appear green and red, respectively (Figure 5). The PCL fibers had mostly live cells on the surface, indicated by the stretched morphology of the green cells. In contrast, the 5 wt% $AgNO_3$ PT 5 fibers showed no live cells, and red cells appeared to have a spherical morphology, further indicating death. The NaOH rinsed 5 wt% $AgNO_3$ PT 5 surfaces had regions where very healthy live cells were present (Figure 6C) and regions where dead cells appeared (Figure 5D). The percent of live and dead cells were calculated over an approximately 0.4 cm^2 area (Figure 6) for each fiber treatment condition as well. It is clear that the Saos-2 cells best adhered to the control PCL fibres, as the average percent live cells was 80.6% ± 6.2%, and significantly less cells adhered to the 5 wt% $AgNO_3$ fibers as they only had 40.7% ± 12% live cells. The NaOH rinsed fibers had an average percent live cells in-between the range of both the PCL and 5 wt% $AgNO_3$ fibers, being 61.1% ± 20.4%. Interestingly, the NaOH rinsed fibers had significantly less percent live cells than the PCL ($p < 0.05$), however, had significantly more live cells ($p < 0.05$) than the 5 wt% Ag NO_3 fibers. The large standard deviation observed in the NaOH percent live cells is expected, as in fluorescence microscopy images, the fibers appeared to have some areas with many live cells and others that were more barren.

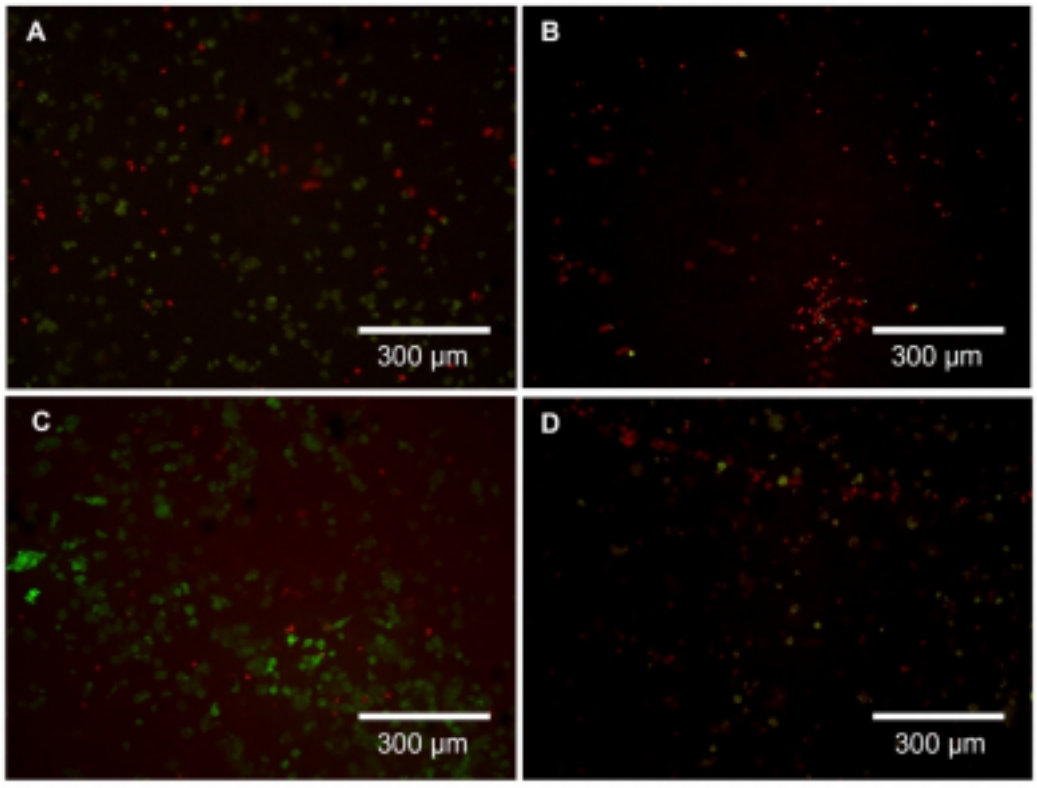

Figure 5. Live/Dead images of Saos-2 cells cultured on control and treated fibers for 24 hours, where green and red represents live and dead cells, respectively. (a) control PCL fibers (b) 5 wt% $AgNO_3$ PT 5 fibers and (c, d) 5 wt% $AgNO_3$ PT 5 fibers previously rinsed with NaOH for 1 day. Areas of the NaOH rinsed fibers appear to have growth similar to the control, while other areas have low growth.

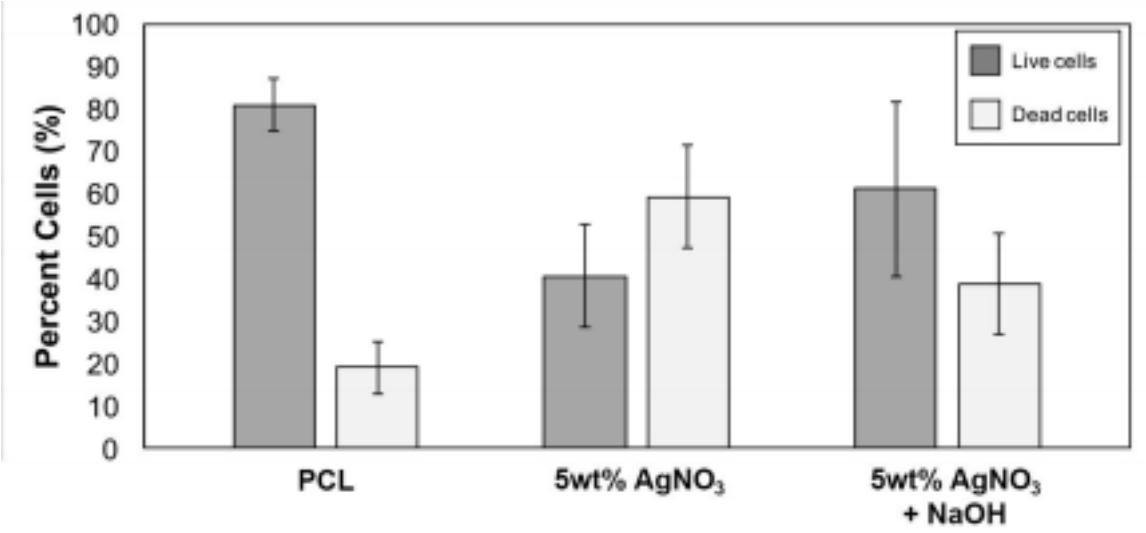

Figure 6. Percent live and dead Saos-2 cells based on live/dead images of cells cultured on PCL control 5 wt% $AgNO_3$, and NaOH rinsed 5 wt% $AgNO_3$ fibers. The amount of live cells is significantly different for each fiber treatment ($p < 0.05$).

Discussion

Fiber and Ag NP Fabrication

Electrospun scaffolds for tissue regeneration applications attempt to mimic the native tissue ECM. As the native bone ECM (the collagen matrix) is on the nano-length scale [32], efforts were placed on reducing the fiber diameter of the PCL scaffold materials produced in this work. Smaller electrospun fibers have been speculated to be related to solvent selection, whereby the use of more harmful solvents tends to result in the decrease in fiber diameter [17,33]. However, we achieved the complete dissolution of PCL in acetone, a less harmful alternative to other organic solvents. While larger diameter fibers are associated with such a solvent, trace amounts of the solution solvent may be found in subsequently fabricated fibrous meshes, thus the use of a more harmful solvent could cause adverse effects. Although the electrospun fibers initially produced in our work showed fiber diameters of approximately 1.5 μm, potentially because acetone was the solvent, we applied two methods to further decrease the fiber diameter of our final PCL electrospun meshes.

First, we preloaded the solutions with varying wt% (1, 2.5, 5, and 10) of $AgNO_3$ prior to electrospinning, which was thought to contribute to fiber diameter reduction, as the addition of biosynthesized silver NPs to PCL solutions previously achieved nano-sized

PCL fibers [10]. However, such pre-loading effects were not seen with our PCL/$AgNO_3$ fibers, as fiber diameters remained statistically similar (Figure 1E).

Secondly, we employed air plasma treatment to decrease fiber diameter while simultaneously reducing the preloaded $AgNO_3$ to Ag NPs. Fiber diameters were impacted by air plasma treatment as increasing plasma treatment time from 1 to 10 minutes for all of the PCL/$AgNO_3$ fibers resulted in a statistically significant decrease in fiber diameter ($p < 0.05$). Fiber diameters were significantly reduced by plasma treatment because highly energetic ions in air plasma can break carbon-carbon bonds in the polymer and produce small volatile organic fragments, resulting in etching of the fiber [34]. The reduction seems to be limited though, as there was no significant difference between those that were air plasma treated for 5 and 10 minutes for the PCL/$AgNO_3$ fibers. Additionally, the diameter of the PCL fibers lacking any $AgNO_3$ significantly decreased with all increasing air plasma treatment times (1, 5 and 10 minutes; $p < 0.05$). These observations suggest that the addition of the $AgNO_3$ slows the etching effect of the air plasma treatment, and perhaps $AgNO_3$ even reinforces polymer integrity, as no significant diameter decrease was observed among any of the plasma treatment times for the 10 wt% groups. However, with 10 wt% $AgNO_3$, 30 minutes of air plasma treatment completely etched the fibers.

In previous works, various plasma gases including ArO_2 have been utilized to reduce silver on thin films and electrospun nanofibers [25,35] and etch polymeric fibers [25]. This study demonstrates the effectiveness of air plasma, which is arguably a more efficient method for silver reduction than a pure gas system. Air plasma is effective at this reduction because the ions present lead to the reduction of silver. Reduction of $AgNO_3$ was observed by Annur et al. after ArO_2 plasma treatment of $AgNO_3$ containing electrospun chitosan fibers through the use of X-ray photoelectron spectroscopy (XPS) analysis[25]. In our work, the formation of Ag NPs using air plasma treatment was confirmed *via* TEM imaging (Figure 2), where NPs were on average 7 ± 4 nm in diameter. Similarly to our study, Annur et al. also observed a decrease in fiber diameter as a function of plasma treatment time; however, significant fiber diameter losses were also noted with increasing preloading of $AgNO_3$[25]. Meanwhile, the loss of PCL mass in this work was most likely due to the formation of small volatile organic molecules due to the breaking of C-C bonds in the polymer by the oxygen or nitrogen reactive ions.

Surface Treatments

The aforementioned antimicrobial properties of Ag NPs are ultimately favourable for the elimination of bacterial colonies, however Ag NPs have also been demonstrated to be toxic to mammalian cultures[36].In this work, we employed two surface modification techniques to increase the wettability, alter the surface chemistry, and modify the fibre morphology to increase the biocompatibility of the fibres, despite the presence of Ag NPs. The surface was first modified with air plasma treatment, which both reduced the $AgNO_3$ precursor to NPs and etched the fibre surface. Plasma treatment from a variety of sources, including ArO_2, N_2+H_2, and NH_3+O_2 is known to both etch PCL surfaces

resulting in a decrease of C and an increase of O and N containing surface groups such as amines, alcohols and carboxylic acids [37]. This ultimately leads to the increased wettability of surfaces, which in turns has the potential to increase cellular attachment.

Fibers were subsequently subjected to a 0.1 M NaOH rinse for 24 hours. NaOH has shown to also increase the wettability of PCL as it can hydrolyze the ester bonds in PCL, creating carboxyl groups on the surface [26]. Interestingly, unlike other works that have experimented with shorter NaOH submersion times at higher NaOH concentrations [26,30], our SEM images show a morphology change of the fibres. It appears that the NaOH rinse changed the fibre morphology to a more agglomerated structure in random locations on the surface. The topographic changes due to this alkaline degradation is suspected to also influence cellular attachment and proliferation on these surfaces. Fibers subjected to NaOH rinses were tested against *S. pneumoniae* to determine if the rinse decreased the efficacy of the Ag NPs, and their biocompatibility was assessed against Saos 2 cells.

Antibacterial Properties

Smaller Ag NPs (*i.e.* < 10 nm), such as those generated through air plasma treatment, are able to act as potent antimicrobial agents as they release silver ions, Ag^+ with the additional benefit that their small size can penetrate the cell membrane, contributing to bacterial colony elimination [38]. The success of the surface immobilized Ag NPs against *S. pneumoniae* was demonstrated as colonies were only established in a perimeter around the silver doped nanofibres after 24 hours of incubation. Notably, areas of inhibition were not statistically different when S. pneumoniae came into contact with nanofibers regardless of whether or not the samples were NaOH rinsed ($p < 0.05$), demonstrating that the NaOH rinse did not dissolve the AgNPs. Overall, these results suggest that the AgNP containing electrospun meshes may be effective at inhibiting bacterial growth directly on an implant surface. The non-plasma treated fibres containing only $AgNO_3$ presented a clear radius of inhibition, with a statistically significant larger area of inhibition when compared to all other tested fibres ($p < 0.05$). This can be attributed to the fact that the $AgNO_3$ is not surface immobilized, allowing it to leach from the fibres and therefore have a larger effective area. This ultimately suggests that the $AgNO_3$ containing fibres have exhibited a burst Ag^+ release effect, meanwhile the Ag NP containing meshes have a slow Ag^+ release, which is more optimal for long term implant materials.

Biocompatibility

A major concern when introducing Ag NPs or any Ag functionalized coating into biomedical devices is the potential cytotoxicity it can introduce to host or mammalian cells. The uptake of Ag NPs ranging from 10 nm – 100 nm in diameter by mammalian cells such as red blood cells and lung cells can induce changes in cell morphology, function, or even apoptosis with large doses[36]. Similar effects are seen with $AgNO_3$ accumulation as well, but $AgNO_3$ can also impact gene development in *in vivo* models[39]. To mitigate these cytotoxic effects, the fibres were surface treated with air

plasma treatment, followed by an NaOH rinse, as described above. Fluorescence microscopy and subsequent image analysis revealed that although the NaOH rinsed fibers had significantly fewer ($p < 0.05$) live cells than the control, it still maintained significantly ($p < 0.05$) more Saos-2 cellular attachment than the fibres containing the NPs (the 5 wt% $AgNO_3$ fibres). This suggests that although some cytotoxicity is introduced via the addition of Ag NPs to the fibres, the NaOH recovers some of the overall biocompatibility. One limitation to this assessment is that dead cells can be washed away during sample preparation for fluorescence microscopy, making the number of dead cells ultimately uncertain. Additionally, cellular function cannot be assessed through live/dead assays, and therefore further in vitro or in vivo testing is needed to fully evaluate the biocompatibility of the fibres. The bioresorbable nature of PCL, enhanced by the air plasma treatment, presents challenges for assessing viability of adherent cells over longer periods of time (up to one week) in cell media. Our attempts at this testing showed rapid fibre degradation or detachment from the sample surface. Evaluating the fibres in vivo in a confined zone between implant and bone would be the most representative of the behaviour of the PCL as both an antibacterial, and bioresorbable osteconductive material.

Conclusion

In this work, electrospinning was employed to create continuous PCL fibers loaded with $AgNO_3$. The $AgNO_3$ was then reduced using a simple one-step air plasma treatment to create surface-immobilized AgNPs. Air plasma treatment was shown to significantly reduce the fiber diameter of control PCL fibers, as well as that of the fibers preloaded with 1, 2.5 and 5 wt%$AgNO_3$ when comparing times of 1 minute to 5 and 10 minutes. Ag NP containing fibers demonstrated statistically similar antibacterial inhibition against *S. pneumoniae* growth upon contact in comparison to NaOH rinsed Ag NP containing fibres, suggesting the surface morphology and chemistry changes induced by the NaOH rinse did not affect the antimicrobial properties of the fibres. Saos-2 cellular activity was more prominent on Ag NP containing fibres rinsed with NaOH, however less than the control PCL fibres, suggesting the NaOH rinse maintained the antibacterial properties of the fibres, while recovering some biocompatibility properties. This study demonstrated the effectiveness of air plasma treatment as a straightforward method to generate surface immobilized Ag NPs through a one-step reduction reaction of $AgNO_3$ for use in bone engineering applications. Future work to determine the adhesion properties of the material to standard implant substrates including titanium alloys would be of interest. Finally, longer term *in vitro* or *in vivo* studies are needed to assess the sustained effects the material on biological tissues.

Acknowledgements

DMB was supported by an NSERC USRA, and DMB, BEJL, and SS were partially supported by Ontario Graduate Scholarships. This research was supported by NSERC Discovery Grants to KG and JMM. JMM is the recipient of an Early Researcher Award from the province of Ontario and is the holder of the Tier 2 Canada Research Chair in Micro- and Nanostructured Materials. We thank Prof. Dawn Bowdish for access to her antibacterial testing laboratory, Justin Boyle for his assistance with antibacterial testing, Helen Luu for assistance with making of agar plates, and Michelle Shah for assistance with bacterial plate imaging. SEM was performed at the Canadian Centre for Electron Microscopy a facility supported by NSERC and other governmental sources. TEM was performed at the McMaster Faculty of Health Sciences Electron Microscopy Facility, we gratefully acknowledge Marcia Reid for her assistance. Mammalian cell studies were performed at the Biointerfaces Institute, at McMaster.

References

[1] Goodman S B, Yao Z, Keeney M and Yang F 2013 The future of biologic coatings for orthopaedic implants *Biomaterials***34** 3174–83

[2] Carlsson L, Röstlund T, Albrektsson B, Albrektsson T and Brånemark P I 1986 Osseointegration of titanium implants. *Acta Orthop. Scand.***57** 285–9

[3] Ribeiro M, Monteiro F J and Ferraz M P 2012 Infection of orthopedic implants with emphasis on bacterial adhesion process and techniques used in studying bacterial-material interactions. *Biomatter***2** 176–94

[4] Franci G, Falanga A, Galdiero S, Palomba L, Rai M, Morelli G and Galdiero M 2015 Silver Nanoparticles as Potential Antibacterial Agents *Molecules***20** 8856–74

[5] Garcia-Contreras R. Argueta-Figueroa L, Mejoa-Rubalcava C, Jimenez-Martinez R, Cuevas-Guajardo S, Sanchez-Reyna P A and Mendieta-Zeron H 2011 Perspectives for the use of silver nanoparticles in dental practice *Int. Dent. J.***61** 297–301

[6] Prabhu S and Poulose E K 2012 Silver nanoparticles: mechanism of antimicrobial action, synthesis, medical applications, and toxicity effects *Int. Nano Lett.***2** 32

[7] You C. Han C, Wang X, Zheng Y, Li Q, Hu X and Sun H 2012 The progress of silver nanoparticles in the antibacterial mechanism, clinical application and cytotoxicity *Mol. Biol. Rep.***39** 9193–201

[8] Arakawa H, Neault J F and Tajmir-Riahi H A 2001 Silver(I) complexes with DNA and RNA studied by Fourier transform infrared spectroscopy and capillary electrophoresis. *Biophys. J.***81** 1580–7

[9] Dong H, Wang D, Sun G and Hinestroza J P 2008 Assembly of metal nanoparticles on electrospun nylon 6 nanofibers by control of interfacial hydrogen bonding interactions *Chem. Mater.***20** 6627–32

[10] Augustine R, Kalarikkal N and Thomas S 2015 Electrospun PCL membranes incorporated with biosynthesized silver nanoparticles as antibacterial wound dressings *Appl. Nanosci.***6** 337-344

[11] Jia Y T, Liu Q, Q and Zhu X Y 2011 Preparation of Ultrafine Poly(*ε Caprolactone*) Fibers Containing Silver Nanoparticles via Electrospinning Method *Adv. Mater. Res.***332**–**334** 1235–8

[12] Xu X, Yang Q, Wang Y, Yu H, Chen X and Jing X 2006 Biodegradable electrospun poly(l-lactide) fibers containing antibacterial silver nanoparticles *Eur. Polym. J.***42** 2081–7

[13] Wang Y, Yang Q, Shan G, Wang C, Du J, Wang S, Li Y, Chen X, Jing X and Wei Y 2005 Preparation of silver nanoparticles dispersed in polyacrylonitrile nanofiber film spun by electrospinning *Mater. Lett.***59** 3046–9

[14] Yoo H S, Kim T G and Park T G 2009 Surface-functionalized electrospun nanofibers for tissue engineering and drug delivery *Adv. Drug Deliv. Rev.***61** 1033–42

[15] Pham Q P, Sharma U and Mikos A G 2006 Electrospinning of polymeric nanofibers for tissue engineering applications: a review. *Tissue Eng.***12** 1197–211

[16] Abedalwafa M, Wang F, Wang L and Li C 2013 Biodegradable poly-epsilon caprolcaction (PCL) for tissue engineering applications: A review *Rev. Adv. Mater. Sci***34** 123–40

[17] Hasan M, Nayem K A, Hossain M B and Nahar S 2014 Production of Tissue Engineering Scaffolds from Poly Caprolactone (PCL) and Its Microscopic Analysis **3** 39–43

[18] Han D and Gouma P-I 2006 Electrospun bioscaffolds that mimic the topology of extracellular matrix *Nanomedicine Nanotechnology, Biol. Med.***2** 37–41

[19] Jang J H, Castano O and Kim H W 2009 Electrospun materials as potential platforms for bone tissue engineering *Adv. Drug Deliv. Rev.***61** 1065–83

[20] Fang R, Zhang E, Xu L and Wei S 2010 Electrospun PCL/PLA/HA based nanofibers as scaffold for osteoblast-like cells. *J. Nanosci. Nanotechnol.***10** 7747– 51

[21] Repanas A, Wolkers WF, Gryshkov O, Miller M G B Pcl/Peg Electrospun Fibers as Drug Carriers for the Controlled Delivery of Dipyridamole *Silico Vitr. Pharmacol.***1** 1-10

[22] Abdal-Hay A, Hwang M G and Lim J K 2012 In vitro bioactivity of titanium implants coated with bicomponent hybrid biodegradable polymers *J. Sol-Gel Sci. Technol.***64** 756–64

[23] Catauro M, Papale F and Bollino F 2015 Characterization and biological properties of TiO2/PCL hybrid layers prepared via sol–gel dip coating for surface modification of titanium implants *J. Non. Cryst. Solids***415** 9–15

[24] Matena J, Petersen S, Gieseke M, Teske M, Beyerbach M, Kampmann A, Escobar H, Gellrich N-C, Haferkamp H and Nolte I 2015 Comparison of Selective Laser Melted Titanium and Magnesium Implants Coated with PCL *Int. J. Mol. Sci.***16** 13287–301

[25] Annur D, Wang Z, Liao J and Kuo C 2015 Plasma-Synthesized Silver Nanoparticles on Electrospun Chitosan Nanofiber Surfaces for Antibacterial Applications *Biomacromolecules***10** 3248-55

[26] Cao Z, Wang D, Lyu L, Gong Y and Li Y 2016 Fabrication and characterization of PCL/$CaCO_3$ electrospun composite membrane for bone repair *RSC Adv.***6** 10641–9

[27] Rasband W. ImageJU.S. National Institutes of Health. Maryland USA [28] Xue J, He M, Liu H, Niu Y, Crawford A, Coates P D, Chen D, Shi R and Zhang L 2014 Drug loaded homogeneous electrospun PCL/gelatin hybrid nanofiber structures for anti-infective tissue regeneration membranes *Biomaterials***35** 9395– 405

[29] Lee B E J, Exir H, Weck A and Grandfield K 2018 Characterization and evaluation of femtosecond laser-induced sub-micron periodic structures generated on titanium to improve osseointegration of implants *Appl. Surf. Sci.***441** 1034–42

[30] Hernandez A R, Contreras O C and Acevedo L O 2013 Poly(ε-caprolactone) Degradation Under Acidic and Alkaline Conditions *Am. J. Polym. Sci.***3** 70–5

[31] Park J ., Kim J ., Lee S J, Lee S G, Jeong Y K, Kim S E and Lee C 2007 Surface hydrolysis of fibrou poly(e-caprolactone) scaffolds for enhanced osteoblast adhesion and proliferation *Macromol. Res.***15** 424–9

[32] Mouw J K, Ou G and Weaver V M 2014 Extracellular matrix assembly: a multiscale deconstruction. *Nat. Rev. Mol. Cell Biol.***15** 771–85

[33] Li L, Li G, Jiang J, Liu X, Luo L and Nan K 2012 Electrospun fibrous scaffold of hydroxyapatite/poly (ε-caprolactone) for bone regeneration. *J. Mater. Sci. Mater. Med.***23** 547–54

[34] Morent R, De Geyter N, Desmet T, Dubruel P and Leys C 2011 Plasma Surface Modification of Biodegradable Polymers: A Review *Plasma Process. Polym.***8** 171–90

[35] Fortunati E, Mattioli S, Visai L, Imbriani M, Fierro J L G, Kenny J M and Armentano I 2013 Combined effects of Ag nanoparticles and oxygen plasma treatment on PLGA morphological, chemical, and antibacterial properties. *Biomacromolecules***14** 626–36

[36] Gliga A R, Skoglund S, Wallinder I O, Fadeel B and Karlsson H L 2014 Size dependent cytotoxicity of silver nanoparticles in human lung cells: the role of cellular uptake, agglomeration and Ag release. *Part. Fibre Toxicol.***11** 11

[37] Yan D, Jones J, Yuan X Y, Xu X H, Sheng J, Lee J C-M, Ma G Q and Yu Q S 2013 Plasma treatment of electrospun PCL random nanofiber meshes (NFMs) for biological property improvement *J. Biomed. Mater. Res. Part A***101A** 963–72

[38] Li R, Chen J, Cesario T C, Wang X, Yuan J S and Rentzepis P M 2016 Synergistic reaction of silver nitrate, silver nanoparticles, and methylene blue against bacteria. *Proc. Natl. Acad. Sci. U. S. A.***113** 13612–7

[39] Poynton H C, Lazorchak J M, Impellitteri C A, Blalock B J, Rogers K, Allen H J, Loguinov A, Heckman J L and Govindasmawy S 2012 Toxicogenomic Responses of Nanotoxicity in *Daphnia magna* Exposed to Silver Nitrate and Coated Silver Nanoparticles *Environ. Sci. Technol.***46** 6288–96